First DNP Results from a Liquid Water-TEMPOL Sample at 400 MHz and 260 GHz

M. J. Prandolini, V. P. Denysenkov, M. Gafurov, S. Lyubenova, B. Endeward, M. Bennati[*], and **T. F. Prisner**

Institute of Physical and Theoretical Chemistry, Center for Biomolecular Magnetic Resonance, J. W. Goethe University Frankfurt, Frankfurt am Main, Germany

Abstract. Using a newly designed liquid-state dynamic nuclear polarization (DNP) spectrometer operating at a magnetic field of 9.2 T, a DNP enhancement of $-4.0(1)$ was achieved for protons in a liquid water-TEMPOL sample. The DNP mechanism was observed to be the Overhauser effect, where the polarization was transfered via electron–proton dipolar relaxation. At full microwave power, the sample was heated by 17 K above room temperature, causing a significant increase in the DNP enhancement. These first results from the Frankfurt liquid-state DNP spectrometer represent a significant step towards the application of DNP to large biomolecules in the liquid state.

1 Introduction

The early development of liquid-state dynamic nuclear polarization (DNP) was performed at low magnetic fields, where the Overhauser effect (OE) [1] was found to be most effective. Other DNP mechanisms, such as solid effect (SE), thermal mixing (TM), or cross effect (CE), also initially studied at low magnetic fields, are effective in the solid state [2, 3]. The progress towards high-field DNP of large biomolecules in aqueous solutions has been restricted for two reasons. Firstly, in the 1960s it was predicted that the DNP enhancement of the OE at higher magnetic fields (over 3 T) rapidly decreases to zero [4]. Thus, with the development of high-field liquid-state nuclear magnetic resonance (NMR) spectrometers, DNP was not considered a viable option. The second reason is the large dielectric losses of water at high microwave (MW) frequencies [5], which cause considerable sample heating due to the electric field and greatly reduce the quality factor, Q, of MW cavities. For example, at 260 GHz the skin depth of pure water

---

[*] Present address: Max Planck Institute for Biophysical Chemistry, Göttingen, Germany

is about 0.2 mm. The solution to this latter problem is the use of MW resonant cavities, which spatially separate the electric and magnetic fields (for details of our MW cavity and DNP spectrometer see ref. 6). The past situation of liquid-state DNP at low magnetic fields was summarized in two review articles [7, 8].

On the other hand, in the solid state there has been considerable progress towards high-field DNP on large biomolecules by Griffin's group at Massachusetts Institute of Technology [9]. The DNP mechanisms TM and CE, involving a three-spin process (i.e., dipolar-coupled two electron spins and a nuclear spin), were shown to have considerable efficiency at high magnetic fields. Recently, even larger DNP enhancements were achieved by directly exploiting the three-spin process using biradicals [10], i.e., strongly coupling the two free electrons in a single molecule. Furthermore, in the solid state at low temperatures (about 77 K), the dielectric losses of water are greatly reduced. Under the requirements of magic-angle spinning and sample volume for good NMR sensitivity, the present design of the solid-state MW structure has a low quality factor, $Q \sim 1$, and therefore, the success of these experiments depends on using high-power gyrotrons as MW sources [11].

Whereas the three-spin CE produces large solid-state DNP enhancements at high magnetic fields, this has not been shown for liquids, where almost exclusively the OE has been studied. In summary, the OE enhancement ε is usually factorized into

$$\varepsilon = \xi f s \frac{\gamma_S}{\gamma_I}, \tag{1}$$

where ξ is the DNP coupling constant, f is the leakage factor ($f = 1 - T_1/T_{1w}$, where T_1 and T_{1w} are the nuclear–spin relaxation with and without free radicals), s is the degree of electron spin saturation, and γ_S and γ_I are the gyromagnetic ratios of the electron and nucleus, respectively. In the case of protons the maximum enhancement is 658, assuming the other parameters are unity (i.e., ξ, f, $s = 1$). Using equations (31) and (37) from ref. 7, Fig. 1 shows the dependence of the coupling constant, ξ, on the product $\omega_S \tau$, where ω_S is the electron spin frequency and τ is the correlation time, for scalar and dipolar coupling mechanisms. As an example, at the electron spin Larmor frequency of 260 GHz and relatively short correlation times ($\tau = 25$ ps), the OE is close to zero for pure dipole–dipole relaxation (Fig. 1). However, when scalar coupling is dominant, large enhancements are possible if other relaxation pathways are kept to a minimum.

The first attempt at challenging the conventional wisdom that the OE is not efficient at high magnetic fields was performed by Griffin's group. Signal enhancements of 180, 40, -36 and 8.4 were achieved on the isotopes ^{31}P in Ph$_3$P, ^{13}C in CCl$_4$, ^{15}N in C$_6$H$_5$NH$_2$, and ^{19}F in C$_6$F$_6$, respectively. This experiment was performed on a 5 T DNP spectrometer using a deuterated benzene solution with radical 1,3-bisdiphenylene-2-phenylallyl (BDPA) [12]. The positive sign of the enhancement (γ_S is negative and γ_I is positive for all nuclei except for ^{15}N) indicated that scalar coupling was the dominant relaxation process. However for ^{1}H
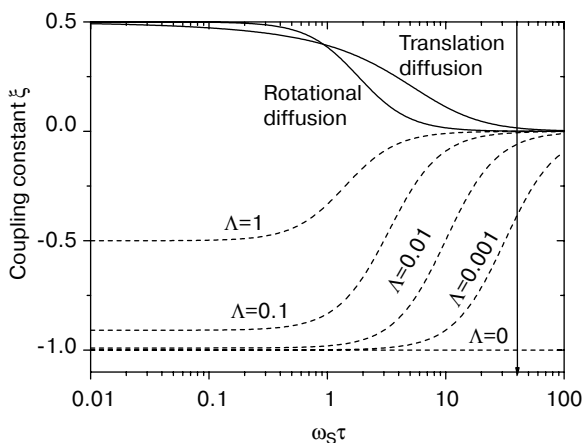
Fig. 1. Liquid-state DNP coupling constant, ξ, as a function of the product, $\omega_S\tau$. The two solid lines model the dipole–dipole relaxation mechanism for translational and rotational diffusion. The dashed lines model scalar relaxation, where Λ describes the amount of leakage coming from a time-dependent electron spin relaxation. The vertical line at $\omega_S\tau = 40$ is the product of 260 GHz times a correlation time of 25 ps, which corresponds to our experimental conditions.

nuclei, a small negative enhancement of only -0.5 due to electron–nuclear dipolar relaxation was observed. These results show that DNP with scalar interactions works also at high magnetic fields but requires specific interactions between the radical and solvent. Additionally, it might be difficult to transfer the polarization of such nuclei to large biomolecules.

For high-field liquid-state DNP, we therefore propose a strategy whereby protons of the aqueous solvent are directly polarized. This polarization can be transfered by spin diffusion or using pulse techniques onto the protons of large biomolecules. The challenging part of this strategy is the initial step of polarizing the solvent. As part of an European Design Study BIO-DNP, a DNP spectrometer operating at 9.2 T was constructed to explore this experimentally (see ref. 6). In this paper, the first results from a liquid water-TEMPOL sample are presented. Unexpected large DNP proton enhancements via the OE through dipole–dipole relaxation were observed. The effects of MW heating were observed, increasing the enhancement even further at higher MW power levels. Possible modifications to the experimental setup to further improve the DNP enhancement are discussed. These results represent a significant step towards liquid-state DNP of large biomolecules.

2 NMR Performance with the Application of MW

To measure the amount of MW heating and demonstrate the performance of the double-frequency resonator described in ref. 6, NMR of a distilled water sample

was measured, where the chemical shift dependence on temperature is known (0.009(1) ppm/°C [13]). The water solution was taken up into a quartz capillary, purchased from Polymicro, with an inner diameter (i.d.) of 0.05 mm and an outer diameter (o.d.) of 0.15 mm. The capillary was then placed along the axis of the helix double resonator and held in place by movable plungers at either end. The helix double resonator serves as both an NMR-tuned coil and an MW cavity. The maximum incident power MW at the cavity was measured to be approximately 22 mW, and the microwave cavity ($Q = 410$) was critically matched to the transmission system (see ref. 6 for more details). After tuning the MW cavity to mode TE$_{011}$ at 260 GHz, the distance between the plungers was approximately 1.6 mm, resulting in a sample size of 3 nl. Thereafter, an NMR spectrum of the water sample was taken with and without MW (Fig. 2).

In Fig. 2, the peak on the left-hand side was from water molecules inside the MW cavity. MW heating caused a decrease in the chemical shift of 0.15 ppm of the main peak, resulting in an estimated temperature increase of 17 K. In addition, the total line width increased by 33% upon the application of MW, while the integrated NMR signal size remained the same. The broadening was caused by a distribution of electric MW fields inside the sample. Naturally, the protons within water molecules are magnetically equivalent and therefore resonate at a single NMR line. The multiplicity of NMR water peaks is due to the construction details of the double resonator and the differences in magnetic susceptibility of the surrounding materials. Water molecules within the radio frequency (rf) helix coil, however, lying outside the cavity, experience different local fields and are shifted to the right, compared to water molecule inside the cavity. The peaks on the right-hand side are from water molecules outside the cavity and therefore experienced no direct MW heating, resulting in a negligible chemical shift (see Fig. 2).
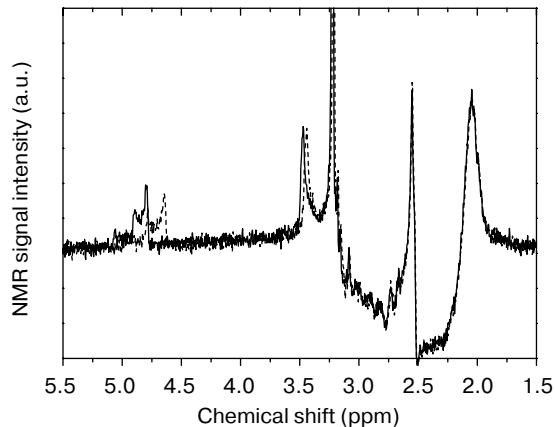

Fig. 2. NMR signal of pure water with and without MW at full power (22 mW). The signal on the left-hand side came from water inside the MW cavity and was shifted as a result of MW heating. The larger peaks on the right-hand side came from water molecules outside the MW cavity, but still inside the helix (see the text).

For these first experiments on our newly developed liquid-state DNP spectrometer, the aim was to test the overall electron paramagnetic resonance (EPR) (see ref. 6) and NMR performance, and most importantly, demonstrate the feasibility of performing DNP on water-based liquid samples. Therefore, no attempt was made to optimize either the B_0, B_1 or B_2 field homogeneity over the liquid sample. The performance of the spectrometer and the DNP enhancement can therefore be greatly improved by further technological developments as is outlined in the outlook of this paper.

3 First DNP Experimental Results on a Water-TEMPOL Sample

The sample contains 6.4 mM 4-hydroxy-TEMPO 97% (TEMPOL), purchased from Sigma-Aldrich, dissolved in distilled water. The solution was placed in a quartz capillary (i.d., 0.05 mm; o.d., 0.15 mm) and the MW cavity was tuned to a TE_{011} mode. Since the ratio of solvent to TEMPOL protons was about 1000, no attempt was made to detect the proton NMR signal from TEMPOL. The EPR spectrum is split by the hyperfine interaction with the nitrogen nucleus (^{14}N, $I = 1$) into three lines. The MW source was then tuned to the central EPR line and the sample was irradiated while recording the NMR spectrum. An NMR free induction decay (FID) signal was taken consisting of 8 scans with the time between pulses of 12 s, which was well above the proton $T_1 = 0.75(2)$ s. The NMR spectrum was taken as a function of the MW power. Note that only the NMR signal resulting from the solution within the MW cavity is shown in Fig. 3.

With increasing MW power, a number of effects were observed. Firstly, the line position was shifted linearly with the MW power. Half of the power (3 dB
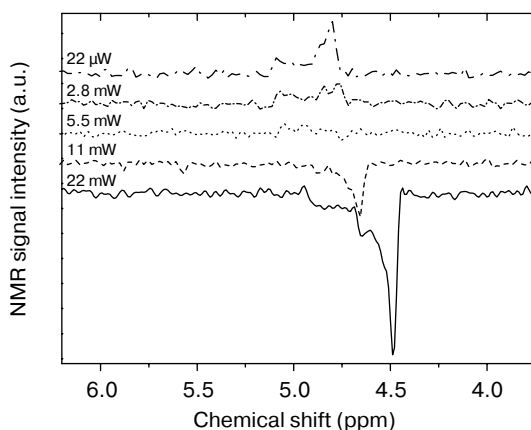

Fig. 3. NMR signal of 6.4 mM TEMPOL in distilled water with varying MW power. The MW frequency was tuned to the central EPR line of TEMPOL. Each spectrum has a level vertical shift to make each spectrum easily distinguishable. The NMR spectrum at 22 μW (30 dB attenuation) was considered to be the reference signal without MW and a maximum DNP enhancement of −4.0(1) was achieved at 22 mW.

attenuation) corresponded to approximately half-maximum of the chemical shift (Fig. 3). With pure water as a calibration standard, the maximum shift at 22 mW represented an increase in the sample temperature by 17 K above room temperature (293 K). Secondly, a negative DNP enhancement was observed with increasing MW power. The DNP enhancement was calculated from $\varepsilon = (\nu_{MW} - \nu_0)/\nu_0$, where ν_{MW} was the integrated NMR signal with MW and ν_0 was a reference integrated NMR signal without MW, in this case at maximum attenuation (22 µW). At maximum power (0 dB attenuation), the DNP enhancement was estimated to be $-4.0(1)$ at 310 K. Thirdly, the DNP enhancement was not uniform across the NMR line shape, as a result of the nonuniformity of the magnetic MW field. The MW field is zero at the ends of the cavity and maximum in the center. This was particularly evident by comparing the NMR signals at MW powers of 22 µW and 2.8 mW, where the central peak was greatly reduced compared with the left-hand shoulder with increasing power. The line broadening due to variations in the MW electric field intensity was discussed in Sect. 2.

When complete saturation of the EPR signal cannot be achieved, it is common to plot the inverse of the DNP enhancement factor as a function of the inverse of the power (Fig. 4). This plot generally gives a straight line whose intercept at "infinite" power is equal to the inverse of the maximal enhancement at EPR saturation [8]. The main deviations from a linear relation can be caused by heating with the MW power [14]. At higher MW powers, the temperature increases, reducing the correlation time and thereby increasing the DNP enhancement above a linear response. A maximum (EPR-saturating) enhancement of $-1.5(1)$ was estimated from a linear fit to the last four points between 0.1 and 0.2 mW^{-1}, where the temperature changes less than 3.5 K above room tem-
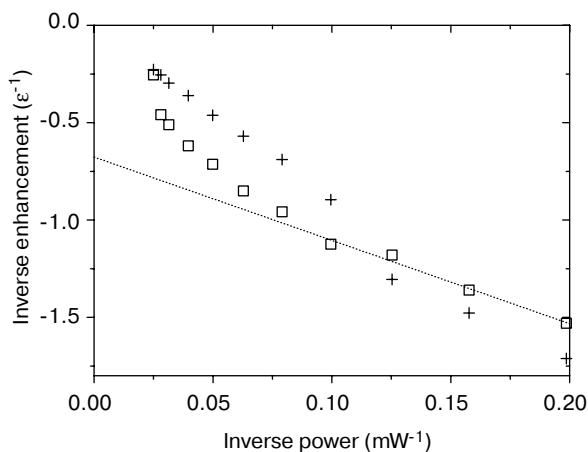

Fig. 4. Inverse DNP enhancement of 6.4 mM TEMPOL in distilled water as a function of inverse power was determined using two methods. The squares represent integrated NMR signals, while the crosses represent the peak amplitude of the NMR line. A linear fit to the last four square points, between 0.1 and 0.2 mW^{-1}, is also shown. A maximum inverse DNP enhancement of $-1/1.5(1)$ was estimated by extrapolating this line to the saturating power.
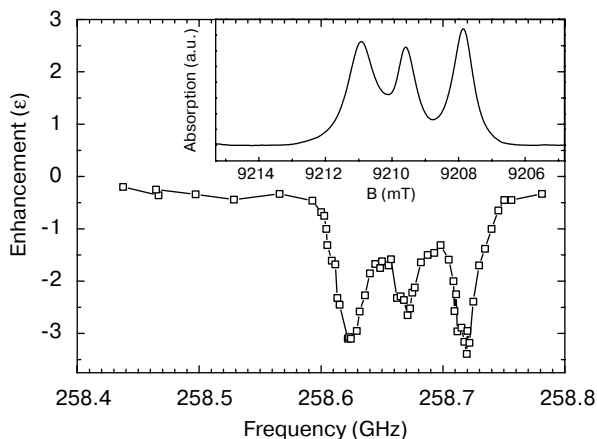
Fig. 5. DNP enhancement of 6.4 mM TEMPOL in distilled water as a function of MW frequency at maximum power of about 22 mW. The inset is the corresponding EPR response, in this case the EPR spectrum was taken using a traditional magnetic field sweep (see ref. 6 for details).

perature. The different inverse power dependence of the integrated NMR signal and the peak amplitude might reflect the inhomogeneous MW field distributions, where the peak of the NMR line corresponded to the water molecules at the center of the cavity, where the MW field is the highest.

Additionally, a plot of the DNP enhancement as a function of the MW frequency is given in Fig. 5, the inset shows the corresponding absorption EPR spectrum (discussed in ref. 6). Firstly, a negative DNP enhancement was observed across the complete EPR line, which confirmed that the DNP mechanism was caused by OE, via electron–nuclear dipole–dipole relaxations. Scalar-dominated relaxation would produce a positive enhancement [7] (Fig. 1). Other mechanisms such as SE, TM or CE would cause another field-dependent form of the enhancement across the EPR line, i.e., for these mechanisms, pumping at the center of the electron spin spectra produces no DNP, and off-center excitations produce negative (positive) DNP for MW frequencies above (below) the EPR signal [2]. Secondly, the amplitudes of the DNP enhancement as a function of frequency corresponded to the relative amplitudes of the EPR spectrum as a function of field. Thus the maximum enhancement was achieved at an MW frequency corresponding to the excitation of the last hyperfine line.

4 Discussion and Outlook

At 310 K, a DNP enhancement of $-4.0(1)$ was observed in a water-TEMPOL solution. This value was observed below saturation, and thus still higher values can be expected if EPR could be saturated. However, close to room temperature (293 K), the estimated maximum DNP enhancement at saturating power was $-1.5(1)$ (Fig. 4). To the best of our knowledge, these values are the largest en-

hancements produced on water protons in the liquid state at high magnetic fields. These values were determined by integrating over the NMR water signal. Because the MW field is nonuniform across the sample (i.e., MWs are zero at the ends of the cavity and maximum at the center) and additionally spin diffusion from the highly polarized water molecules at the center of the cavity to the edges might reduce polarization, we can expect that both of the above DNP enhancements represent rather lower estimates of the real values, for the given temperature and level of the electron saturation.

The DNP enhancement for this sample also has a very strong temperature dependence; the enhancement more than doubles with a temperature increase of 17 K. Heating increases the molecular motion and thereby reduces the correlation time, τ. From the negative sign of the DNP enhancement, the dominant mechanism was via electron–proton dipole–dipole relaxation (see Fig. 1). In comparison to the previously mentioned DNP results at 5 T [12], various nonproton nuclei, including ^{19}F in C_6F_6, were found to have a scalar-dominated DNP mechanism, while the proton enhancement (-0.5) was dipolar-dominated. The smaller proton enhancement, compared with our results, was most likely due to the greater size of the organic solvent compared to water, and thereby a larger correlation time τ. At the present state of knowledge, we cannot exclude a mixture of scalar and dipolar effects, partially canceling each other out.

To achieve reliable estimates of the saturation factor, s in Eq. (1), DNP measurements should be performed with changing radical concentration and different hyperfine couplings by replacing ^{14}N with ^{15}N [15]. Therefore no reliable direct estimates for the coupling factor ξ can be made in this paper. Nuclear magnetic relaxation dispersion (NMRD) has been used to estimate correlation times τ for a given motional model (spectral density function) [7]. These data can be used to predict ξ at higher magnetic fields. Recent NMRD measurements on TEMPOL in water at room temperature estimated τ to be between 15 to 20 ps [16], other estimates give 73 ps measured on a similarly sized nitroxide [17]. Using the spectral density function for translational motion from ref. 7, and assuming $s = f = 1$; maximum estimates of ε vary from 2.9 (at $\tau = 73$ ps) to 21 (at $\tau = 17$ ps). These values can also greatly vary using other spectral density functions (for example see ref. 14). Clearly, at high magnetic fields given the past technical problems there is a lack of reliable data and accurate motional models.

Development of hardware and sample preparation is in steady progress. If an isolated droplet of sample could be positioned within the cavity where MWs are relatively homogeneous, a number of improvements become possible. Firstly, this will eliminate the spurious NMR peaks coming from water molecules outside the cavity (Fig. 2). Secondly, the integrated DNP enhancement increases by increasing the average MW field over the sample. Thirdly, spin diffusion to protons outside the MW fields is eliminated. And fourthly, line broadening due to a distribution of electric field heating is reduced. Additionally, progress is being made on improving the double-resonance structure and transmission system.

Finally, these initial experiments from the Frankfurt liquid-state DNP spectrometer demonstrated the feasibility of achieving usable DNP polarization transfers from electron spins to protons in aqueous solutions at moderate free radical

concentrations using OE. The final transfer of polarization onto the target bio-molecule can be achieved either passively by spin diffusion or actively using pulse sequences.

Acknowledgments

References

 1. Overhauser, A.W.: Phys. Rev. **92**, 411 (1953)
 2. Wind, R.A., Duijvestijn, M.J., van der Lugt, C., Manenschijn, A., Vriend, J.: Prog. Nucl. Magn. Reson. Spectrosc. **17**, 33 (1985)
 3. Atsarkin, V.A.: Sov. Phys. Usp. **21**, 725 (1978)
 4. Hausser, K.H.: Z. Phys. **183**, 265 (1965)
 5. Jackson, J.D.: Classical Electrodynamics, 3rd edn. Wiley, New York (1999)
 6. Denysenkov, V.P., Prandolini, M.J., Krahn, A., Gafurov, M., Endeward, B., Prisner, T.F.: Appl. Magn. Reson. **34**, 289–299 (2008)
 7. Hausser, K.H., Stehlik, D.: Adv. Magn. Reson. **3**, 79 (1968)
 8. Müller-Warmuth, W., Meise-Gresch, K.: Adv. Magn. Reson. **11**, 1 (1983)
 9. Hall, D.A., Maus, D.C., Gerfen, G.J., Inati, S.J., Becerra, L.R., Dahlquist, F.W., Griffin, R.G.: Science **276**, 930 (1997)
10. Hu, K.-N., Yu, H.-H., Swager, T.M., Griffin, R.G.J.: Am. Chem. Soc. **126**, 10844 (2004)
11. Bajaj, V.S., Hornstein, M.K., Kreischer, K.E., Sirigiri, J.R., Woskov, P.P., Mak-Jurkauskas, M.L., Herzfeld, J., Temkin, R.J., Griffin, R.G.: J. Magn. Reson. **189**, 251 (2007)
12. Loening, N.M., Rosay, M., Weis, V., Griffin, R.G.: J. Am. Chem. Soc. **124**, 8808 (2002)
13. Wu, T., Kendell, K.R., Felmlee, J.P., Lewis, B.D., Ehman, R.L.: Med. Phys. **27**, 221 (2000)
14. Wind, R.A., Ardenkjaer-Larsen, J.-H.: J. Magn. Reson. **141**, 347 (1999)
15. Armstrong, B.D., Han, S.: J. Chem. Phys. **127**, 104508 (2007)
16. Höfer, P., Parigi, G., Luchinat, C., Carl, P., Guthausen, G., Reese, M., Carlomagno, T., Griesinger, C., Bennati, M.: J. Am. Chem. Soc. **130**, 3254–3255 (2008)
17. Borah, B., Bryant, R.G.: J. Chem. Phys. **75**, 3297 (1981)

Authors' address: Mark Prandolini, Institute of Physical and Theoretical Chemistry, J. W. Goethe University Frankfurt, Max-von-Laue-Strasse 7, 60438 Frankfurt am Main, Germany
E-mail: prandolini@chemie.uni-frankfurt.de